



Free Vibration Analysis of Functionally Graded Porous Nano-plates with Different Shapes Resting on Elastic Foundation

Trac Luat Doan¹, Pham Binh Le², Trung Thanh Tran³, Vu Khac Trai⁴, Quoc Hoa Pham⁵

¹ Faculty of Mechanical Engineering, Le Quy Don Technical University, Hanoi, Vietnam, Email: doanluat@lqdtu.edu.vn

² Faculty of Mechanical Engineering, Le Quy Don Technical University, Hanoi, Vietnam, Email: lephambinh@lqdtu.edu.vn

³ Faculty of Mechanical Engineering, Le Quy Don Technical University, Hanoi, Vietnam, Email: trantrungthanh@lqdtu.edu.vn

⁴ Automobile Enterprise, 751 One Member Limited Liability Company, Ho Chi Minh City, Vietnam, Email: vkt751@gmail.com

⁵ Department of Training, Tran Dai Nghia University, Ho Chi Minh City, Vietnam, Email: phamquochoa@tdttu.edu.vn

Received December 25 2020; Revised February 28 2021 ; Accepted for publication February 28 2021.

Corresponding author: Q.H. Pham (phamquochoa@tdttu.edu.vn)

© 2021 Published by Shahid Chamran University of Ahvaz

Abstract. This paper proposes a finite element method (FEM) based on a nonlocal theory for analyzing the free vibration of the functionally graded porous (FGP) nano-plate with different shapes lying on the elastic foundation (EF). The FGP materials with two-parameter are the power-law index (k) and the porosity volume fraction (\varnothing) in two cases of even and uneven porosity. The EF includes Winkler stiffness (k_1) and Pasternak stiffness (k_2). Some numerical results in our work are compared with other published to verify accuracy and reliability. Moreover, the influence of geometric parameters, materials on the free vibration of the FGP nano-plates resting on the EF is comprehensively investigated.

Keywords: Nano-plates, FG material, Nonlocal elasticity theory, Elastic foundation.

1. Introduction

Nowadays, with the strong development of technology and science, the research of nano-structure has always been deeply interested in scientists around the world. However, studies showed that classical plate theory for structures of millimeters or above is inaccurate for nanometer-sized structures. To solve this problem, many theories have been suggested such as the modified couple stress theory [1], the strain gradient theory [2], and the nonlocal theory [3], [4]. Among these theories, the nonlocal theory [3], [4] is preferred due to their simplicity and accuracy. For example, Li and co-workers [5] proposed a new nonlocal model to analyze the static bending and dynamic response for circular elastic nano-solids. Ansari and his colleagues [6] analyzed the free vibration of the nano-graphene plates. Arash [7] reviewed recent research studies on the application of the nonlocal theory in modeling carbon nanotubes and graphene. Farajpour et al. [8] examined thermomechanical vibration of nano-plates including surface effects. Jalali and co-workers [9] employed a molecular dynamics method to calculate the effect of out-of-plane defects on the vibration of graphene plates. Moreover, applying the nonlocal theory to investigate the various performances of nano-plates/shells also found in refs. [10]-[20]. Besides, Tran et al. [21] calculated mechanical behavior of FGP nanoshells by extend four-unknown higher-order shear deformation nonlocal theory. Tran and co-workers [22] employed the finite difference method to investigate static bending and free vibration of the sandwich functionally graded nanoplates. Liu et al. [23] analyzed dispersion characteristics of guided waves in FGM micro/nanoplates using the modified couple stress theory. In addition, Phung-Van and his colleagues investigated static/dynamic of functionally graded carbon nanotube-reinforced composite nanoplates based on the nonlocal strain gradient isogeometric model [24] and the nonlocal elastic continuous isogeometric model [25]. Zheng et al. [26] examined the bending, buckling, and free vibration of rectangular nanoplates using an up-to-date symplectic superposition method. Ho and co-workers [27] investigated the effect of Negative Poisson's ratios on the mechanical properties of nanoplates.

Recently, the application of FG materials has been widely spread in nanostructures such as thin films [28], [29], fully released nano-electro-mechanical system (NEMS) [30] due to their excellent performance. Hence, investigating the mechanical behaviors of the FG material nanostructures has become the subject of attention of many researchers. Simsek [31] employed the Galerkin method to study the free vibration of axially FG tapered nanorods. And in [32], he examined the static bending and buckling of the FG nano-beam based on the Timoshenko theory. Natarajan and his colleagues [33] studied the free vibration of FG nano-plates based on isogeometric analysis (IGA). Applying the analytical solution, Nazemnezhad [34] computed the nonlinear free vibration of FG nano-beams, and Hashemi et al. [35], [36] studied the nonlinear free vibration of piezoelectric FG nano-beams. Natarajan and his colleagues [37] investigated the vibration of FG nano-plates relied on the Mori-Tanaka homogenization scheme. Jung et al. [38] employed Navier's solution to study the mechanical behavior of the Sigmoid FGM nano-plates. Nami and co-workers [39] investigated the thermal buckling of FG nano-plates by using third-order shear deformation theory (TSDT). Hashemi and co-



workers [40] calculated free vibration of circular/annular FGM nano-plates by employing the analytical method (AM). Salehipour and his colleagues [41], [42], presented the AM for the free vibration analysis of the FG micro/nano-plates based on the three-dimensional elasticity theory. Ansari and his co-workers [43] proposed a new differential quadrature method (DQM) to analyze the bending static and free vibration of FG nano-plates. From the analysis of the above literature, most of them used analytical solutions to present behaviors of FG nano-plates. However, the analytical method is limited when the geometry model, boundary conditions, or types of the load becomes more complex. As an alternative, numerical methods can be developed to fill the gap in these problems.

With the analysis of nano-structures resting on the EF, some typical works are published such as Wang et al. [44] computed the static bending of the nano-plates lying on the EF. Narendar et al. [45] investigated the wave dispersion of a single-layered graphene sheet embedded in an elastic polymer matrix. Pouresmaeli et al. [46] studied the vibration behaviors of nano-plates resting on the viscoelastic medium. Zenkour et al. [47] calculated thermal buckling of nano-plates on the EF by using the sinusoidal shear deformation theory. Daikh et al. [48] analyzed bending of FG nano-plates placed on EF using the higher-order shear deformation plate theory and nonlocal strain gradient theory. Ebrahimi and his colleagues [49] employed nonlocal strain gradient theory to analyze the wave propagation of smart magnetostrictive sandwich nanoplates (MSNPs). Panyatong and his colleagues [50] based on nonlocal theory and surface stress to study the bending behavior of nano-plates on the EF and so on.

Nowadays, the applying of artificial intelligence (AI) in science as well as in mechanical problems are being a new trend. Professor Rabczuk's research team presented novel ideas to solve inverse acoustics problems which based purely on artificial neural network (ANN) [51]; deep neural network (DNN) [52]; the machine learning (ML) [53] apply in the mechanical field and naturally account for uncertainties. Furthermore, the authors provide a Matlab code for the uncertainty analysis to help extract the material parameters needed for simulations [54]. Zhuang et al. [55] developed a deep autoencoder based on the energy method (DAEM) to investigated the bending, buckling, and free vibration of thin plates. The numerical results show the effectiveness of their proposed method. It is a new advance in analyzing the mechanical behavior of structures.

According to the best of the authors' knowledge, the free vibration analysis of FGP nano-plates resting on EF mainly uses the analytical method. As mentioned above, the exact solution is very difficult to conduct when the geometry model, boundary conditions, and loads are complication. Therefore, to overcome this limitation, the eight-node quadrilateral (Q8) element combining with the nonlocal theory to accurately describe the stress-strain and displacement field of the FG nano-plates with different shapes resting on the EF is investigated in this work. The proposed method is verified by comparing with those of other available results in the literature. Moreover, the effects of input parameters on the free vibration behavior of the FGP nano-plates are comprehensively investigated.

To achieve a self-contained paper with enhanced readability, this paper is organized as follows. Section 1 is a general introduction. We present finite element formulations base on the nonlocal theory of free vibration analysis of FGP nano-plates resting on the EF in Sections 2 and 3. The numerical results of free vibration are discussed in Section 4. Section 5 gives some major conclusions.

2. Theoretical formulation

2.1 Schematic of FGP nano-plates

In this paper, we use four schematics of nano-plates include Square nano-plate (Fig.1a), L-shaped nano-plate (Fig.1b), Annular nano-plate (Fig.1c), and Half-annular nano-plate (Fig.1d). These are the normally models widely used in extremely small electronic devices such as CPUs, transistors, and so on.

The FGP materials with the variation of two-constituents and two different distributions of porosity through-thickness are determined as follows [56]:

$$\text{Case 1: } P(z) = P_m + (P_c - P_m) \left(\frac{z}{h} + 0.5 \right)^k - \frac{\xi}{2} (P_c + P_m) \tag{1}$$

$$\text{Case 2: } P(z) = P_m + (P_c - P_m) \left(\frac{z}{h} + 0.5 \right)^k - \frac{\xi}{2} (P_c + P_m) \left(1 - \frac{2|z|}{h} \right)$$

with case 1 and case 2 are the modified mixture rule for the two-constituents FG plate with even porosity and uneven porosity, respectively. P_c and P_m are respectively the typical material properties at the top (ceramic) and the bottom surfaces (metal). k is the power-law index, ξ ($\xi \leq 1$) represents the porosity volume fraction. Figs. 2(a)-2(b) show elastic modulus E of FGP material (Al/Al_2O_3) in two cases of even and uneven porosity with the porosity volume fraction $\xi = 0.2$. Distribution material properties through-thickness of nano-plates is also presented in Figs. 3(a)-3(d) when the power-law index gets values $k=0, 1, 2, 4$.

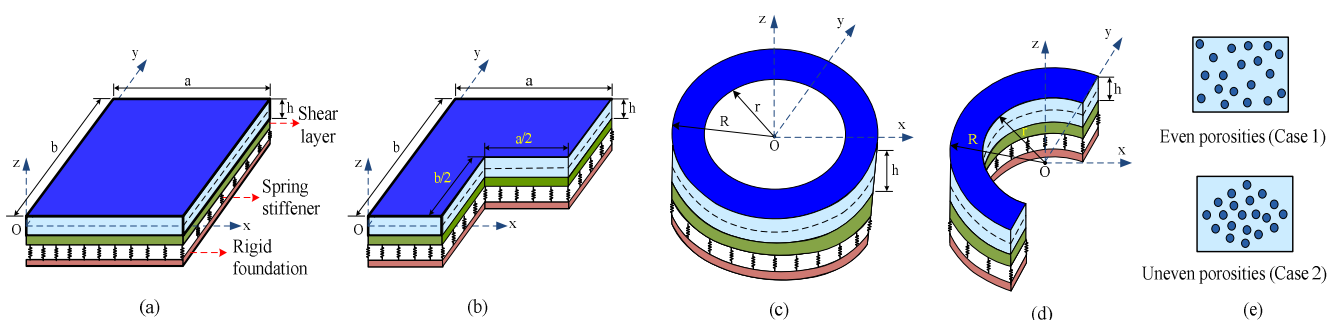


Fig. 1. Modeling the FGP nano-plate with two cases of porosity distribution resting on EF in the global coordinate OXYZ. (a) Square nano-plate, (b) L-shaped nano-plate, (c) Annular nano-plate, (d) Half-annular nano-plate, (e) Porosities distribution.



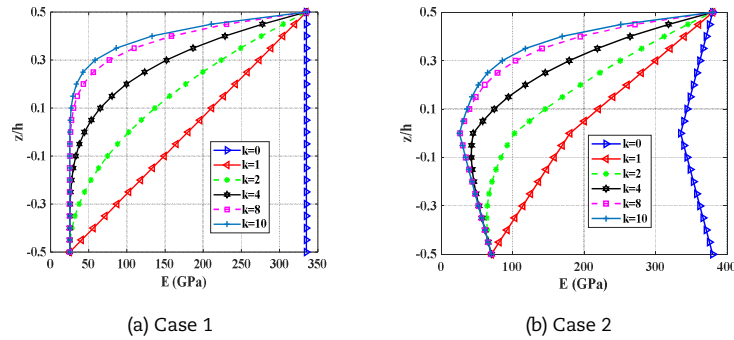


Fig. 2. Elastic modulus E of FGP material (Al/Al₂O₃) with different power-law index k. (a) Even porosity (case 1), (b) Uneven porosity (case 2).

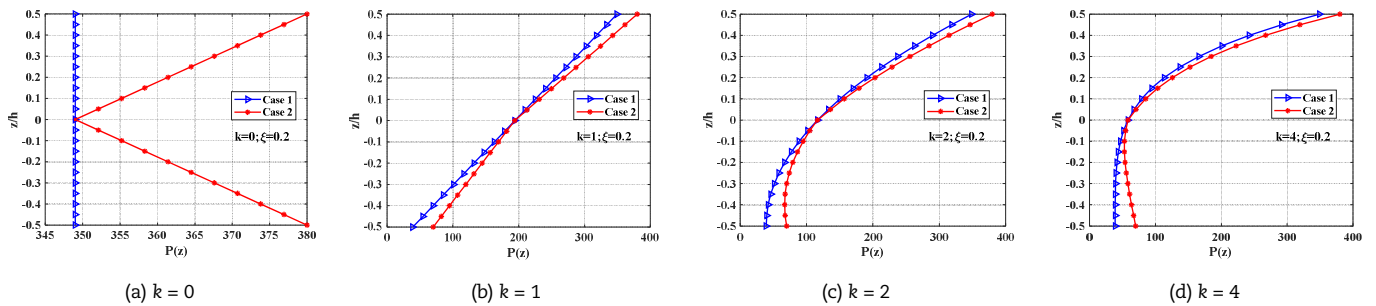


Fig. 3. Distributions material property through-thickness of FGP nano-plates. (a) k = 0, (b) k = 1, (c) k = 2, (d) k = 4.

The reaction–deflection relation of the EF is given by [47]:

$$q_e = k_1 w - k_2 \nabla^2 w \tag{2}$$

with $\nabla^2 = \frac{\partial^2}{\partial x^2} + \frac{\partial^2}{\partial y^2}$ and w is the displacement of the nano-plate following z -axis; k_1, k_2 are respectively Winkler stiffness and Pasternak stiffness.

2.2 Nonlocal elasticity theory

Following the nonlocal theory, the relation stress-strain is determined as follows [3], [4]:

$$\sigma - \mu \nabla^2 \sigma = \mathbf{Q}; \quad \mu = (e_0 l)^2 \tag{3}$$

in which: μ is nonlocal factor (the small scale effect), l is an internal characteristic length and $e_0 = const$. When $l = 0$, the nonlocal theory degenerates into the classical elasticity theory. \mathbf{Q} is the stress tensor at a point which is calculated via the local theory as:

$$\mathbf{Q} = \mathbf{D} \cdot \boldsymbol{\varepsilon} \tag{4}$$

where

$$\boldsymbol{\varepsilon} = \begin{Bmatrix} \varepsilon_{xx} \\ \varepsilon_{yy} \\ \varepsilon_{xy} \\ \varepsilon_{xz} \\ \varepsilon_{yz} \end{Bmatrix}; \quad \boldsymbol{\sigma} = \begin{Bmatrix} \sigma_{xx} \\ \sigma_{yy} \\ \sigma_{xy} \\ \sigma_{xz} \\ \sigma_{yz} \end{Bmatrix} \tag{5}$$

$$\mathbf{D} = [C_{ijkl}] = \begin{bmatrix} \mathbf{D}_b & \mathbf{0}_{3 \times 2} \\ \mathbf{0}_{2 \times 3} & \mathbf{D}_s \end{bmatrix} \tag{6}$$

with

$$\mathbf{D}_b = \begin{bmatrix} C_{11} & C_{12} & 0 \\ & C_{22} & 0 \\ sym & & C_{66} \end{bmatrix}; \quad \mathbf{D}_s = \begin{bmatrix} C_{55} & 0 \\ 0 & C_{44} \end{bmatrix} \tag{7}$$



$$C_{11} = C_{22} = \frac{E(z)}{(1-\nu(z))(1+\nu(z))}; C_{12} = \frac{\nu(z)E(z)}{(1-\nu(z))(1+\nu(z))};$$

$$C_{66} = C_{55} = C_{44} = \frac{E(z)}{2(1+\nu(z))}$$
(8)

The displacement field of the nano-plates is expressed as

$$\begin{cases} u(x, y, z) = u_0(x, y) + z\varphi_x(x, y) \\ v(x, y, z) = v_0(x, y) + z\varphi_y(x, y) \\ w(x, y, z) = w_0(x, y) \end{cases}$$
(9)

where: u, v, w are the displacements at point (x, y, z) ; u_0, v_0, w_0 are the displacements at the mid-plane and φ_x, φ_y are the rotation angles of the cross-section around the y -axis, x -axis, respectively.

The deformation field of the FG nano-plate is defined as

$$\boldsymbol{\varepsilon} = \begin{Bmatrix} \varepsilon_{xx} \\ \varepsilon_{yy} \\ \varepsilon_{xy} \\ \varepsilon_{xz} \\ \varepsilon_{yz} \end{Bmatrix} = \begin{Bmatrix} u_{,x} \\ v_{,y} \\ u_{,y} + v_{,x} \\ w_{,x} + u_{,z} \\ w_{,y} + v_{,z} \end{Bmatrix} = \begin{Bmatrix} u_{0,x} \\ v_{0,y} \\ u_{0,y} + v_{0,x} \\ v_{0,x} + \varphi_x \\ w_{0,y} + \varphi_y \end{Bmatrix} + z \begin{Bmatrix} \varphi_{x,x} \\ \varphi_{y,y} \\ \varphi_{x,y} + \varphi_{y,x} \\ 0 \\ 0 \end{Bmatrix}$$
(10)

Eq. (10) may be written by

$$\boldsymbol{\varepsilon} = \begin{Bmatrix} \boldsymbol{\varepsilon}_1 \\ \boldsymbol{\varepsilon}_2 \end{Bmatrix} = \begin{Bmatrix} \boldsymbol{\varepsilon}_1^0 + z\boldsymbol{\varepsilon}_1^1 \\ \boldsymbol{\varepsilon}_2^0 \end{Bmatrix}$$
(11)

with

$$\boldsymbol{\varepsilon}_1 = \begin{Bmatrix} \varepsilon_{xx} \\ \varepsilon_{yy} \\ \varepsilon_{xy} \end{Bmatrix}; \boldsymbol{\varepsilon}_2 = \begin{Bmatrix} \varepsilon_{xz} \\ \varepsilon_{yz} \end{Bmatrix}; \boldsymbol{\varepsilon}_1^0 = \begin{Bmatrix} u_{0,x} \\ v_{0,y} \\ u_{0,y} + v_{0,x} \end{Bmatrix}; \boldsymbol{\varepsilon}_1^1 = \begin{Bmatrix} \varphi_{x,x} \\ \varphi_{y,y} \\ \varphi_{x,y} + \varphi_{y,x} \end{Bmatrix}; \boldsymbol{\varepsilon}_2^0 = \begin{Bmatrix} w_{0,x} + \varphi_x \\ w_{0,y} + \varphi_y \end{Bmatrix}$$
(12)

From Eqs. (11) and (12) the nonlocal force and moment resultants are determined as

$$\begin{Bmatrix} N_{ij} \\ M_{ij} \end{Bmatrix} = \int_{-h/2}^{h/2} \sigma_{ij} \begin{Bmatrix} 1 \\ z \end{Bmatrix} dz; ij = xx, yy, xy$$
(13)

$$\begin{Bmatrix} Q_{xz} \\ Q_{yz} \end{Bmatrix} = \int_{-h/2}^{h/2} \begin{Bmatrix} \sigma_{xz} \\ \sigma_{yz} \end{Bmatrix} dz$$
(14)

Eqs. (13), (14) can be rewritten as

$$\{N_{xy} \quad N_{yy} \quad N_{xy}\}^T = \mathbf{A}\boldsymbol{\varepsilon}_1^0 + \mathbf{B}\boldsymbol{\varepsilon}_1^1$$
(15)

$$\{M_{xy} \quad M_{yy} \quad M_{xy}\}^T = \mathbf{B}\boldsymbol{\varepsilon}_1^0 + \mathbf{X}\boldsymbol{\varepsilon}_1^1$$
(16)

$$\{Q_{xz} \quad Q_{yz}\}^T = \mathbf{A}^s\boldsymbol{\varepsilon}_2^0$$
(17)

where

$$(\mathbf{A}, \mathbf{B}, \mathbf{X}) = \int_{-h/2}^{h/2} \mathbf{D}_b(1, z, z^2) dz; \mathbf{A}^s = \frac{5}{6} \int_{-h/2}^{h/2} \mathbf{D}_s dz$$
(18)

which leads to

$$\begin{Bmatrix} N_{xx} \\ N_{yy} \\ N_{xy} \end{Bmatrix} - \mu \nabla^2 \begin{Bmatrix} N_{xx} \\ N_{yy} \\ N_{xy} \end{Bmatrix} = \mathbf{A}\boldsymbol{\varepsilon}_1^0 + \mathbf{B}\boldsymbol{\varepsilon}_1^1;$$
(19)

$$\begin{Bmatrix} M_{xx} \\ M_{yy} \\ M_{xy} \end{Bmatrix} - \mu \nabla^2 \begin{Bmatrix} M_{xx} \\ M_{yy} \\ M_{xy} \end{Bmatrix} = \mathbf{B}\boldsymbol{\varepsilon}_1^0 + \mathbf{X}\boldsymbol{\varepsilon}_1^1;$$
(20)



$$\begin{Bmatrix} Q_{xz} \\ Q_{yz} \end{Bmatrix} - \mu \nabla^2 \begin{Bmatrix} Q_{xz} \\ Q_{yz} \end{Bmatrix} = \mathbf{A}^s \mathbf{e}_2^0 \quad (21)$$

Using Hamilton's principle, the equation system of the FGP nano-plate are written as follows [57]:

$$N_{xx,x} + N_{xy,y} = J_0 \ddot{u}_0 + J_1 \ddot{\varphi}_x \quad (22)$$

$$N_{xy,x} + N_{yy,y} = J_0 \ddot{v}_0 + J_1 \ddot{\varphi}_y \quad (23)$$

$$Q_{xz,x} + Q_{yz,y} - R = J_0 \ddot{w}_0 \quad (24)$$

$$M_{xx,x} + M_{xy,y} - Q_{xz} = J_1 \ddot{u}_0 + J_2 \ddot{\varphi}_x \quad (25)$$

$$M_{xy,x} + M_{yy,y} - Q_{yz} = J_1 \ddot{v}_0 + J_2 \ddot{\varphi}_y \quad (26)$$

in which R is the active force which combines between the external force in the z -axis and the reaction force of the EF as

$$R = q(x, y) - k_1 w_0 + k_2 \nabla^2 w_0 \quad (27)$$

The mass inertia moment components are determined by the following formulation:

$$(J_0, J_1, J_2) = \int_{-h/2}^{h/2} (1, z, z^2) \rho(z) dz \quad (28)$$

Finally, we perform a few simple calculations by multiplying the equations from Eqs. (22)-(28), respectively with the variables $\delta u_0, \delta v_0, \delta w_0, \delta \varphi_x, \delta \varphi_y$, and integrating on the S_c domain as well as adding together the sides of each equation to obtain the final equation as follows:

$$\int_{S_c} \left(\begin{aligned} & N_{xx} \delta u_{0,x} + N_{xx} (\delta u_{0,y} + \delta v_{0,x}) + N_{yy} \delta v_{0,x} - M_{xx} \delta \varphi_{x,x} + \\ & -M_{xy} (\delta \varphi_{x,y} + \delta \varphi_{y,x}) - M_{yy} \delta \varphi_{y,y} + Q_{xz} (\delta \varphi_x + \delta w_{0,x}) \\ & + Q_{yz} (\delta \varphi_y + \delta w_{0,y}) - (1 - \mu \nabla^2) (q(x, y) - k_1 w_0 + k_2 \nabla^2 w_0) \delta w_0 - \\ & - (1 - \mu \nabla^2) J_2 (\ddot{\varphi}_x \delta \varphi_x + \ddot{\varphi}_y \delta \varphi_y) - (1 - \mu \nabla^2) \left(J_0 (\dot{u}_0 \delta \dot{u}_0 + \dot{v}_0 \delta \dot{v}_0 + \dot{w}_0 \delta \dot{w}_0) + \right. \\ & \left. J_1 (\dot{\varphi}_x \delta \dot{u}_0 + \dot{\varphi}_y \delta \dot{v}_0 + \dot{u}_0 \delta \dot{\varphi}_x + \dot{v}_0 \delta \dot{\varphi}_y) \right) \end{aligned} \right) dx dy = 0 \quad (29)$$

3. Finite Element Formulation

In this study, the eight-node plate element, each node has 5 degrees of freedoms (dofs) are used. The nodal displacement vector can be determined as follows:

$$\mathbf{d}_e = [\mathbf{d}_1^T \quad \mathbf{d}_2^T \quad \mathbf{d}_3^T \quad \mathbf{d}_4^T \quad \mathbf{d}_5^T \quad \mathbf{d}_6^T \quad \mathbf{d}_7^T \quad \mathbf{d}_8^T]^T \quad (30)$$

The displacements at the node i , ($i = \overline{1-8}$) of the element are expressed as

$$\mathbf{d}_i = \{u_{0i} \quad v_{0i} \quad w_{0i} \quad \varphi_{xi} \quad \varphi_{yi}\} \quad (31)$$

The displacement field in the plate element is interpolated through the displacement node as

$$\begin{cases} u_0 = \mathbf{N}_u \mathbf{d}_e; v_0 = \mathbf{N}_v \mathbf{d}_e; w_0 = \mathbf{N}_w \mathbf{d}_e \\ \varphi_x = \mathbf{N}_{\varphi x} \mathbf{d}_e; \varphi_y = \mathbf{N}_{\varphi y} \mathbf{d}_e \end{cases} \quad (32)$$

where $\mathbf{N}_u, \mathbf{N}_v, \mathbf{N}_w, \mathbf{N}_{\varphi x}, \mathbf{N}_{\varphi y}$ are the shape functions:

$$\begin{cases} \mathbf{N}_u = [\mathbf{N}_1^{(1)} \quad \mathbf{N}_2^{(1)} \quad \dots \quad \mathbf{N}_7^{(1)} \quad \mathbf{N}_8^{(1)}]; \\ \mathbf{N}_v = [\mathbf{N}_1^{(2)} \quad \mathbf{N}_2^{(2)} \quad \dots \quad \mathbf{N}_7^{(2)} \quad \mathbf{N}_8^{(2)}]; \\ \mathbf{N}_w = [\mathbf{N}_1^{(3)} \quad \mathbf{N}_2^{(3)} \quad \dots \quad \mathbf{N}_7^{(3)} \quad \mathbf{N}_8^{(3)}]; \\ \mathbf{N}_{\varphi x} = [\mathbf{N}_1^{(4)} \quad \mathbf{N}_2^{(4)} \quad \dots \quad \mathbf{N}_7^{(4)} \quad \mathbf{N}_8^{(4)}]; \\ \mathbf{N}_{\varphi y} = [\mathbf{N}_1^{(5)} \quad \mathbf{N}_2^{(5)} \quad \dots \quad \mathbf{N}_7^{(5)} \quad \mathbf{N}_8^{(5)}]. \end{cases} \quad (33)$$

The matrices $\mathbf{N}_i^{(j)}$ ($j = \overline{1-5}$) in Eq. (33) are given by



$$\begin{cases} \mathbf{N}_i^{(1)} = [\psi_i & 0 & 0 & 0 & 0]; \\ \mathbf{N}_i^{(2)} = [0 & \psi_i & 0 & 0 & 0]; \\ \mathbf{N}_i^{(3)} = [0 & 0 & \psi_i & 0 & 0]; \\ \mathbf{N}_i^{(4)} = [0 & 0 & 0 & \psi_i & 0]; \\ \mathbf{N}_i^{(5)} = [0 & 0 & 0 & 0 & \psi_i]. \end{cases} \tag{34}$$

where ψ_i are the Lagrange interpolation function which is shown in the Appendix.

Substituting Eq. (32) into Eq. (29), the finite element formulation of a typical element can be expressed:

$$\mathbf{M}_e \ddot{\mathbf{d}}_e + \mathbf{K}_e \mathbf{d}_e = \mathbf{F}_e \tag{35}$$

For the free vibration problem:

$$\mathbf{M}_e \ddot{\mathbf{d}}_e + \mathbf{K}_e \mathbf{d}_e = \mathbf{0} \tag{36}$$

with element stiffness matrix is defined as follows:

$$\mathbf{K}_e = \mathbf{K}_e^b + \mathbf{K}_e^s + \mathbf{K}_e^f \tag{37}$$

with $\mathbf{K}_e^b, \mathbf{K}_e^s, \mathbf{K}_e^f$ are the bending, shear element stiffness matrices, and the foundation stiffness matrix, respectively. In which

$$\mathbf{K}_e^b = \int_{S_e} \left(\begin{bmatrix} \mathbf{B}_1^T & \mathbf{B}_2^T \end{bmatrix} \begin{bmatrix} \mathbf{A} & \mathbf{B} \\ \mathbf{B} & \mathbf{X} \end{bmatrix} \begin{bmatrix} \mathbf{B}_1 \\ \mathbf{B}_2 \end{bmatrix} \right) dx dy \tag{38}$$

$$\mathbf{K}_e^s = \int_{S_e} ((\mathbf{B}_2)^T \mathbf{A}^s \mathbf{B}_3) dx dy \tag{39}$$

$$\mathbf{K}_e^f = \int_{S_e} \left(\begin{matrix} k_1 (\mathbf{N}_w^T \mathbf{N}_w + \mu (\mathbf{N}_{w,x}^T \mathbf{N}_{w,x} + \mathbf{N}_{w,y}^T \mathbf{N}_{w,y})) + \\ k_2 \left(\mathbf{N}_{w,x}^T \mathbf{N}_{w,x} + \mathbf{N}_{w,y}^T \mathbf{N}_{w,y} + \right. \\ \left. \mu (\mathbf{N}_{w,xx}^T \mathbf{N}_{w,xx} + \mathbf{N}_{w,yy}^T \mathbf{N}_{w,yy} + \mathbf{N}_{w,xx}^T \mathbf{N}_{w,yy} + \mathbf{N}_{w,yy}^T \mathbf{N}_{w,xx}) \right) \end{matrix} \right) dx dy \tag{40}$$

$$\mathbf{M}_e = \int_{S_e} (\mathbf{N}^T \mathbf{D}_m \mathbf{N} + \mu (\mathbf{N}_{,x}^T \mathbf{D}_m \mathbf{N}_{,x} + \mathbf{N}_{,y}^T \mathbf{D}_m \mathbf{N}_{,y})) dx dy \tag{41}$$

where

$$\mathbf{B}_1 = \begin{bmatrix} \mathbf{N}_{u,x} \\ \mathbf{N}_{v,y} \\ \mathbf{N}_{u,x} + \mathbf{N}_{v,y} \end{bmatrix}; \quad \mathbf{B}_2 = \begin{bmatrix} \mathbf{N}_{\varphi x,x} \\ \mathbf{N}_{\varphi y,y} \\ \mathbf{N}_{\varphi x,x} + \mathbf{N}_{\varphi y,y} \end{bmatrix}; \quad \mathbf{B}_3 = \begin{bmatrix} \mathbf{N}_{w,x} + \mathbf{N}_{\varphi x} \\ \mathbf{N}_{w,y} + \mathbf{N}_{\varphi y} \end{bmatrix}; \tag{42}$$

$$\mathbf{N} = [\mathbf{N}_u^T \quad \mathbf{N}_v^T \quad \mathbf{N}_w^T \quad \mathbf{N}_{\varphi x}^T \quad \mathbf{N}_{\varphi y}^T];$$

$$\mathbf{D}_m = \begin{bmatrix} J_0 & 0 & 0 & J_1 & 0 \\ & J_0 & 0 & 0 & J_1 \\ & & J_0 & 0 & 0 \\ & & & J_2 & 0 \\ & & & & J_2 \end{bmatrix} \tag{43}$$

4. Numerical Results

From the FEM model based on the nonlocal theory, the authors coded a computer program in MATLAB software to check the reliability of the proposed method. The material properties in numerical analyses are presented in Table 1. For convenience, the dimensionless frequencies of the FGP nano-plates are introduced by the following formulations:

$$\Omega = 10\omega h \sqrt{\frac{\rho_m}{E_m}}; \quad K_1 = \frac{k_1 a^2}{D_m}; \quad K_2 = \frac{k_2 a^4}{D_m}; \quad D_m = \frac{E_m h^3}{12(1-\nu^2)}; \tag{44}$$

Table 1. Material properties of the individual materials.

Materials	E (GPa)	ν	ρ (kg/m ³)
Al ₂ O ₃ (ceramic)	380	0.3	3800
Al (metal)	70	0.3	2707



Table 2. The convergence of the natural frequency Ω_1 of the completely simple supported FGM nano-plate ($a/h = 10$).

k	Mesh	4 × 4	6 × 6	8 × 8	10 × 10	12 × 12	[58]
0	Q4	0.0727	0.0617	0.0603	0.0591	0.0588	0.0577
	MITC4	0.0617	0.0587	0.0584	0.058	0.0580	
	Q8	0.0580	0.0578	0.0578	0.0578	0.0577	
1	Q4	0.0572	0.0477	0.0465	0.0454	0.0451	0.0442
	MITC4	0.0473	0.0449	0.0447	0.0444	0.0444	
	Q8	0.0444	0.0443	0.0442	0.0442	0.0442	
4	Q4	0.0484	0.0409	0.04	0.0391	0.0389	0.0381
	MITC4	0.0409	0.0389	0.0387	0.0384	0.0384	
	Q8	0.0384	0.0383	0.0383	0.0383	0.0383	
10	Q4	0.0451	0.0388	0.038	0.0373	0.0372	0.0364
	MITC4	0.0391	0.0372	0.037	0.0368	0.0368	
	Q8	0.0367	0.0366	0.0366	0.0366	0.0366	

Table 3. Natural frequencies $\bar{\omega}$ of the completely clamped isotropic L-shaped plate.

Method	$\bar{\omega}_1$	$\bar{\omega}_2$	$\bar{\omega}_3$	$\bar{\omega}_4$
[59]	1.8832	2.3450	2.7698	3.5714
[60]	1.8395	2.3735	2.7507	3.6030
Present	1.8524	2.3537	2.6918	3.4288

4.1 Convergence and accuracy study

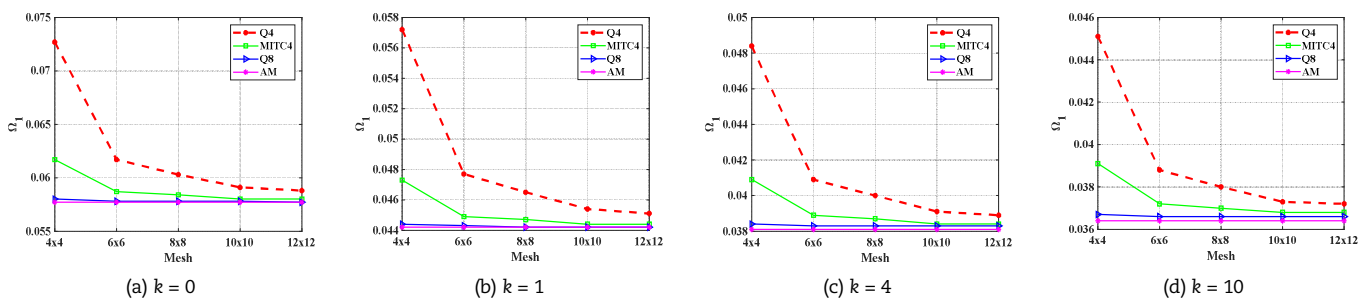
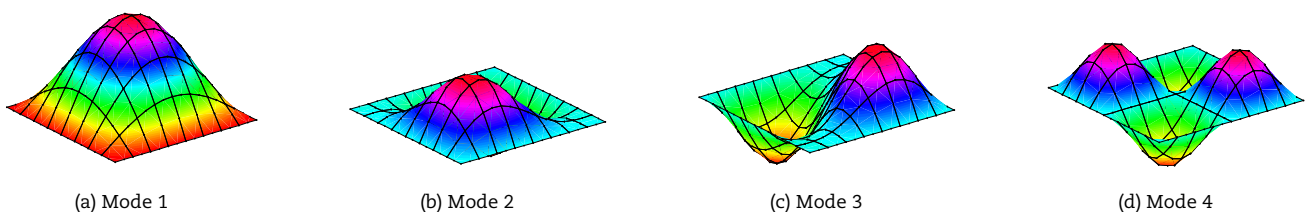
In order to check the accuracy and convergence of the proposed method, the numerical results of the free vibration of the nano-plate are compared with the other published results.

Example 1: we consider a completely simple supported FGM square nano-plate without including nonlocal factor $\mu = 0$. The numerical results with various mesh sizes compared with the AM in [58] are listed in Table 2 and presented in Fig. 4. It can be seen that using the Q8 element converges faster and more accurately than using the mixed interpolation of tensorial components (MITC) for the four-node quadrilateral element (MITC4) and the 4-node quadrilateral (Q4) element. Specifically, using Q8 element with mesh 4×4 is exactly as MITC4 element with mesh 12×12 and more exactly Q4 element with mesh 12×12. For the free vibration problem, with mesh 8×8, numerical results are obtained as accurately as those in the published work of Thai et al. [58]. Therefore, we use mesh 8×8 to investigate the free vibration of FGP nano-plates.

Example 2: The completely clamped L-shaped isotropic plate with $a/h = 10$ (a is fixed), Poisson's ratio $\nu = 0.3$ is considered. The dimensionless frequency is defined $\bar{\omega} = \omega a \sqrt{\rho/G}$ with $G = E/[2(1+\nu)]$. The first four dimensionless frequency of the completely clamped L-shaped plate is listed in Table 3. The present results are compared with the finite-difference technique [59] and isogeometric analysis (IGA) based on the HSDT [60]. It can be concluded that the results of the proposed method are in good agreement with other published works.

4.2 Free vibration problem

For this problem, we consider an FGP nano-plate resting on the EF. Figs. 5, 6 show the first four-mode shapes of FGP square nano-plate has geometric dimensions $a = b = 10$ nm, $h = a/10$ with $K_1 = 100, K_2 = 10, k = 1, \mu = 2, \xi = 0.2$. It can be observed that the second and third mode shapes are similar to each other (the second dimensionless frequency is equal to the third dimensionless frequency). This is suitable for the symmetrical nano-plates under the same supported conditions. With the L-shaped nano-plates, the first four-mode shapes are shown in Figs. 7, 8. It can be seen that the L-shaped nano-plate has higher dimensionless frequencies due to limited boundary conditions. Figs. 9, 10 show the first four-mode shapes of the annular and half-annular FGP nano-plates with geometric dimensions $R = 5$ nm, $r = 2.5$ nm, $h = a/10$. For asymmetric and complex structures (L-shaped, annular, half-annular, and so on) with different boundary conditions, the numerical method proves its great efficiency compared to the analytical method.

**Fig. 4.** The convergence of element mesh to the dimensionless frequency of the FGM nano-plate. (a) $k = 0$, (b) $k = 1$, (c) $k = 4$, (d) $k = 10$.**Fig. 5.** The first four-mode shapes of the completely simple supported FGP (case 1) square nano-plate. (a) 1st mode, $\Omega_1 = 0.8442$; (b) 2nd mode, $\Omega_2 = 1.5156$; (c) 3rd mode, $\Omega_3 = 1.5156$; (d) 4th mode, $\Omega_4 = 1.9983$.

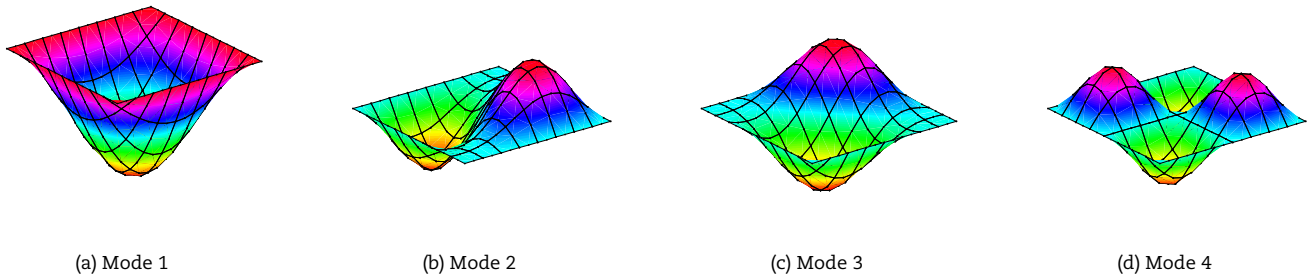


Fig. 6. The first four-mode shapes of the completely simple supported FGP (case 2) square nano-plate. (a) 1st mode, $\Omega_1 = 0.8682$; (b) 2nd mode, $\Omega_2 = 1.5853$; (c) 3rd mode, $\Omega_3 = 1.5853$; (d) 4th mode, $\Omega_4 = 2.091$.

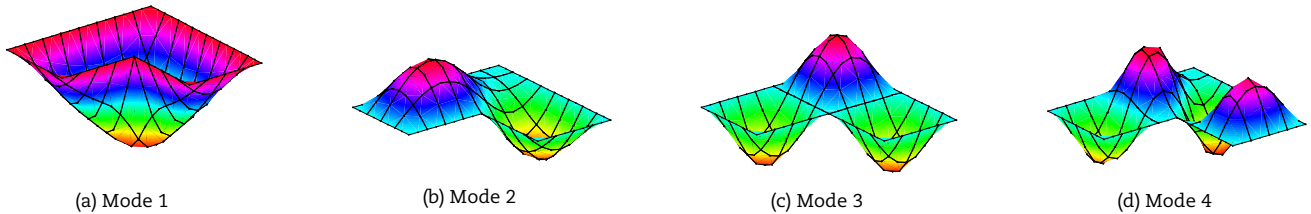


Fig. 7. The first four-mode shapes of the completely simple supported FGP (case 1) L-shaped nano-plate. (a) 1st mode, $\Omega_1 = 1.5102$; (b) 2nd mode, $\Omega_2 = 1.7367$; (c) 3rd mode, $\Omega_3 = 1.9983$; (d) 4th mode, $\Omega_4 = 2.4818$.

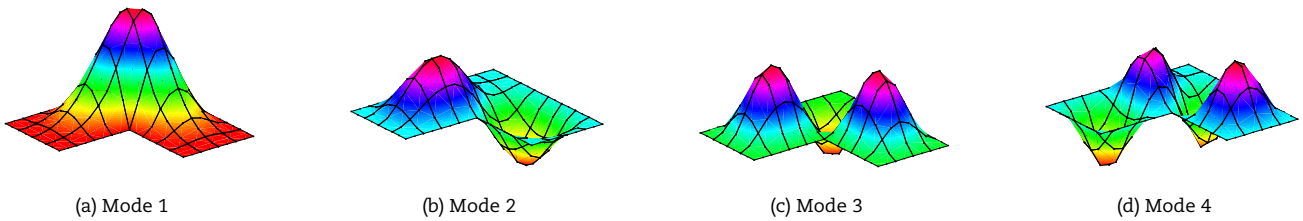


Fig. 8. The first four-mode shapes of the completely clamped FGP (case 1) L-shaped nano-plate. (a) 1st mode, $\Omega_1 = 2.1559$; (b) 2nd mode, $\Omega_2 = 2.4591$; (c) 3rd mode, $\Omega_3 = 2.6306$; (d) 4th mode, $\Omega_4 = 2.9559$.

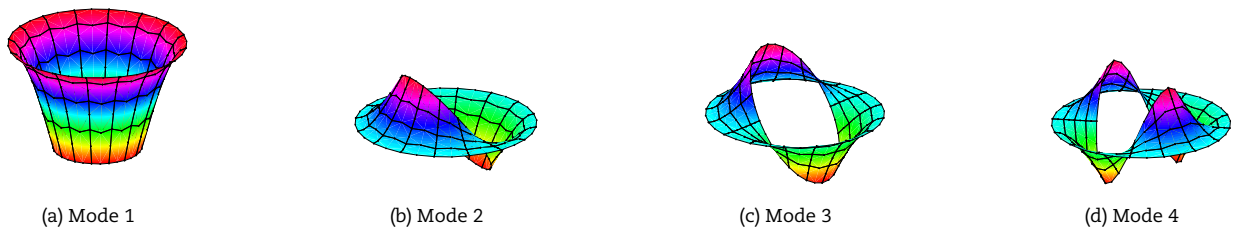


Fig. 9. The first four-mode shapes of the completely clamped FGP (case 1) annular nano-plate. (a) 1st mode, $\Omega_1 = 1.7710$; (b) 2nd mode, $\Omega_2 = 1.9901$; (c) 3rd mode, $\Omega_3 = 1.9901$; (d) 4th mode, $\Omega_4 = 2.4671$.

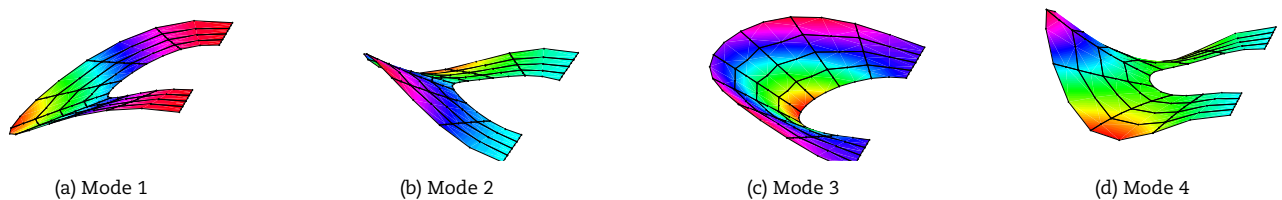


Fig. 10. The first four-mode shapes of the completely clamped FGP (case 1) half-annular nano-plate. (a) 1st mode, $\Omega_1 = 0.6367$; (b) 2nd mode, $\Omega_2 = 1.0892$; (c) 3rd mode, $\Omega_3 = 1.3944$; (d) 4th mode, $\Omega_4 = 1.6566$.

4.2.1. Influence of the parameters of the EF

Firstly, in order to consider the influences of dimensionless parameters of elastic foundation stiffness on free vibration of the FGP square nano-plate, we change K_1 from 100 to 1000, and K_2 from 10 to 100 with respect to $k=1$, $\xi=0.2$, and nonlocal factor gets values $\mu = 0, 1, 2, 4$. The first natural frequencies of the FGP nano-plate with two cases of porosity distribution are presented in Tables 4-5 and shown in Fig. 11. It can be found that when increasing K_1 and K_2 lead to the natural frequency of nano-plates also increase. Furthermore, the effects of the Pasternak foundation (K_2) are stronger than the Winkler foundation (K_1) for all cases of porosity distributions. Specifically, with the same geometry parameters and material properties (see Table 4 with nonlocal factor $\mu = 1$), when $K_2 = 100$ and K_1 increases from 100 to 1000, the first non-dimensional natural frequency increases from 1.4841 to 1.7447 (about 17.6 %), but when $K_1 = 100$ and K_2 only need increase from 10 to 100, the first non-



dimensional natural frequency fast increases from 0.9026 to 1.4841 (about 64,4 %). In addition, the frequencies of the completely clamped (CCCC) FGP nano-plate are greater than the completely simple supported (SSSS) FGP nano-plate. The results are quite reasonable because the simply supported boundary condition is more flexible than the clamped boundary condition.

4.2.2. Influence of the parameters-FGP

Secondly, let us consider the effect of material properties on the free vibration of the FGP square nano-plate. The power-law index k gets values from 0 to 10 and porosity volume fraction ξ changes from 0 to 0.3. We examine the FGP nano-plate resting on EF with the parameters $K_1 = 100, K_2 = 10$ and nonlocal factor $\mu = 0, 1, 2, 4$. Authors only choose the power-law index k in the range (0-10) for investigation because many published works show that when k is greater than 10, the natural frequency of FGP structures does not change much and the recommended value of porosity volume fraction ξ is in the range (0-0.3). The natural frequencies of FGP nano-plate with different boundary conditions are listed in Tables 6-7 and are shown in Figs. 12-13. It can be seen that when k increases, the stiffness of the FGP nano-plate decreases (nano-plate is metal-rich), and hence natural frequencies decrease. We also found that when the increase of nonlocal factor μ leads to natural frequencies of FGP nano-plates decrease. The results are quite reasonable because the increase of the nonlocal factor makes reduce the stiffness of structures in the nonlocal elastic theory. Specifically, with nonlocal factor $\mu = 0$ (classical elastic theory), the natural frequencies of FGP nano-plates are maximum. From Figs. 13(a)-13(g), we can see that with the power-law index $k = 0$ when porosity volume fraction ξ increases, the natural frequencies of FGP nano-plates increase for both cases of porosity distribution. This is because the porosity affects both the stiffness and the mass of nanoshells, this simultaneous interaction causes the natural frequency increase. Besides, the natural frequencies of the FGP nano-plate with porosity distribution of case 1 are larger than the FGP nano-plate with porosity distribution of case 2. With $k > 2$ when ξ increases from 0 to 0.3, the natural frequencies of FGP (case 1) nano-plates decrease, however, the natural frequencies of FGP (case 2) nano-plates are less change and larger than the natural frequencies of FGP (case 1) nano-plates. Basically, the pore appearance in the material reduces the stiffness of the structure. It can be also concluded that the rule of the porosity distribution effects large on the free vibration of FGP nano-plates.

Table 4. Natural frequencies of the SSSS and CCCC FGP (case 1) square nano-plate versus K_1 and K_2 .

Nonlocal factor (μ)	K_2	K_1	SSSS					CCCC				
			100	250	500	750	1000	100	250	500	750	1000
0	10		0.9783	1.0476	1.1538	1.2510	1.3412	1.5338	1.5788	1.6512	1.7205	1.7872
	25		1.1109	1.1723	1.2681	1.3572	1.4408	1.6350	1.6774	1.7457	1.8114	1.8748
	50		1.3022	1.3550	1.4387	1.5177	1.5929	1.7894	1.8282	1.8911	1.9519	2.0109
	75		1.4687	1.5157	1.5910	1.6628	1.7317	1.9299	1.9659	2.0245	2.0815	2.1369
	100		1.6182	1.6610	1.7300	1.7963	1.8602	2.0595	2.0933	2.1484	2.2022	2.2547
1	10		0.9026	0.9773	1.0904	1.1928	1.2871	1.3857	1.4352	1.5141	1.5891	1.6607
	25		1.0228	1.0892	1.1917	1.2861	1.3740	1.4775	1.5241	1.5986	1.6698	1.7381
	50		1.1965	1.2537	1.3437	1.4281	1.5077	1.6179	1.6605	1.7291	1.7952	1.8589
	75		1.3479	1.3990	1.4802	1.5572	1.6305	1.7457	1.7853	1.8494	1.9113	1.9712
	100		1.4841	1.5306	1.6051	1.6764	1.7447	1.8639	1.9010	1.9613	2.0198	2.0766
2	10		0.8442	0.9236	1.0425	1.1492	1.2468	1.2744	1.3279	1.4126	1.4925	1.5683
	25		0.9546	1.0254	1.1337	1.2325	1.3240	1.3588	1.4092	1.4892	1.5652	1.6376
	50		1.1145	1.1758	1.2713	1.3602	1.4436	1.4881	1.5341	1.6080	1.6786	1.7464
	75		1.2542	1.3089	1.3954	1.4768	1.5539	1.6060	1.6488	1.7177	1.7840	1.8479
	100		1.3798	1.4298	1.5093	1.5849	1.6570	1.7151	1.7552	1.8202	1.8828	1.9435
4	10		0.7590	0.8464	0.9748	1.0881	1.1907	1.1167	1.1772	1.2716	1.3594	1.4419
	25		0.8549	0.9333	1.0512	1.1571	1.2540	1.1901	1.2470	1.3365	1.4203	1.4995
	50		0.9944	1.0626	1.1674	1.2636	1.3529	1.3027	1.3549	1.4376	1.5159	1.5903
	75		1.1165	1.1777	1.2731	1.3618	1.4451	1.4057	1.4542	1.5317	1.6053	1.6758
	100		1.2266	1.2825	1.3706	1.4534	1.5317	1.5013	1.5468	1.6198	1.6896	1.7567

Table 5. Natural frequencies of the SSSS and CCCC FGP (case 2) square nano-plate versus K_1 and K_2 .

Nonlocal factor (μ)	K_2	K_1	SSSS					CCCC				
			100	250	500	750	1000	100	250	500	750	1000
0	10		1.0092	1.0692	1.1623	1.2485	1.3291	1.6016	1.6400	1.7022	1.7622	1.8202
	25		1.1245	1.1787	1.2637	1.3434	1.4187	1.6880	1.7245	1.7838	1.8411	1.8967
	50		1.2941	1.3414	1.4167	1.4883	1.5565	1.8218	1.8557	1.9109	1.9645	2.0167
	75		1.4439	1.4865	1.5548	1.6202	1.6831	1.9451	1.9769	2.0288	2.0794	2.1288
	100		1.5796	1.6185	1.6815	1.7422	1.8008	2.0601	2.0901	2.1393	2.1874	2.2344
1	10		0.9297	0.9945	1.0940	1.1851	1.2698	1.4462	1.4885	1.5564	1.6215	1.6841
	25		1.0343	1.0929	1.1842	1.2689	1.3483	1.5247	1.5649	1.6296	1.6919	1.7520
	50		1.1884	1.2398	1.3209	1.3973	1.4698	1.6464	1.6837	1.7440	1.8024	1.8589
	75		1.3247	1.3710	1.4447	1.5149	1.5820	1.7587	1.7937	1.8505	1.9056	1.9591
	100		1.4482	1.4907	1.5588	1.6241	1.6868	1.8636	1.8966	1.9504	2.0028	2.0538
2	10		0.8682	0.9372	1.0422	1.1375	1.2255	1.3293	1.3750	1.4481	1.5176	1.5841
	25		0.9645	1.0271	1.1237	1.2126	1.2954	1.4015	1.4450	1.5147	1.5813	1.6452
	50		1.1064	1.1614	1.2477	1.3283	1.4043	1.5136	1.5540	1.6190	1.6815	1.7417
	75		1.2322	1.2818	1.3604	1.4347	1.5054	1.6173	1.6551	1.7163	1.7754	1.8326
	100		1.3462	1.3918	1.4645	1.5338	1.6001	1.7141	1.7499	1.8079	1.8640	1.9186
4	10		0.7783	0.8547	0.9686	1.0705	1.1635	1.1631	1.2149	1.2967	1.3737	1.4465
	25		0.8621	0.9316	1.0372	1.1329	1.2212	1.2260	1.2753	1.3534	1.4273	1.4976
	50		0.9861	1.0475	1.1423	1.2299	1.3117	1.3238	1.3696	1.4427	1.5122	1.5787
	75		1.0962	1.1517	1.2386	1.3198	1.3963	1.4145	1.4574	1.5263	1.5922	1.6555
	100		1.1962	1.2472	1.3279	1.4039	1.4760	1.4993	1.5399	1.6052	1.6680	1.7285



Table 6. Natural frequencies of the SSSS and CCCG FGP (case 1) square nano-plate versus k and ξ .

Nonlocal factor (μ)	ξ	k	SSSS					CCCG						
			0	2	4	6	8	10	0	2	4	6	8	10
0	0	0	1.2171	0.9272	0.9018	0.8944	0.8878	0.8811	1.9954	1.4548	1.3900	1.3658	1.3473	1.3310
	0.06	0	1.2301	0.9166	0.8873	0.8804	0.8747	0.8688	2.0139	1.4273	1.3534	1.3286	1.3107	1.2949
	0.12	0	1.2445	0.9025	0.8669	0.8602	0.8558	0.8511	2.0344	1.3915	1.3038	1.2781	1.2611	1.2465
	0.18	0	1.2604	0.8830	0.8370	0.8297	0.8268	0.8238	2.0572	1.3434	1.2329	1.2046	1.1892	1.1765
	0.24	0	1.2781	0.8552	0.7904	0.7793	0.7772	0.7764	2.0825	1.2758	1.1229	1.0856	1.0709	1.0615
	0.30	0	1.2980	0.8140	0.7101	0.6829	0.6747	0.6723	2.1110	1.1746	0.9226	0.8422	0.8123	0.7996
1	0	0	1.1170	0.8550	0.8324	0.8259	0.8200	0.8141	1.7996	1.3144	1.2574	1.2363	1.2202	1.2060
	0.06	0	1.1291	0.8460	0.8199	0.8138	0.8088	0.8036	1.8165	1.2900	1.2247	1.2034	1.1879	1.1741
	0.12	0	1.1425	0.8337	0.8021	0.7964	0.7925	0.7884	1.8351	1.2581	1.1805	1.1584	1.1439	1.1313
	0.18	0	1.1573	0.8168	0.7760	0.7697	0.7673	0.7647	1.8558	1.2152	1.1173	1.0929	1.0799	1.0692
	0.24	0	1.1737	0.7926	0.7350	0.7254	0.7238	0.7232	1.8788	1.1550	1.0192	0.9867	0.9744	0.9667
	0.30	0	1.1922	0.7566	0.6644	0.6405	0.6335	0.6316	1.9047	1.0650	0.8414	0.7708	0.7448	0.7339
2	0	0	1.0393	0.7992	0.7788	0.7730	0.7678	0.7624	1.6518	1.2088	1.1574	1.1388	1.1244	1.1116
	0.06	0	1.0507	0.7914	0.7679	0.7625	0.7581	0.7533	1.6673	1.1867	1.1280	1.1090	1.0953	1.0830
	0.12	0	1.0633	0.7808	0.7522	0.7472	0.7438	0.7402	1.6846	1.1579	1.0880	1.0684	1.0557	1.0445
	0.18	0	1.0773	0.7659	0.7291	0.7236	0.7216	0.7194	1.7037	1.1192	1.0308	1.0092	0.9978	0.9885
	0.24	0	1.0928	0.7445	0.6926	0.6842	0.6829	0.6825	1.7250	1.0647	0.9419	0.9130	0.9024	0.8958
	0.30	0	1.1102	0.7126	0.6296	0.6084	0.6022	0.6006	1.7489	0.9834	0.7815	0.7184	0.6953	0.6858
4	0	0	0.9252	0.7179	0.7008	0.6961	0.6917	0.6871	1.4407	1.0589	1.0155	1.0000	0.9880	0.9772
	0.06	0	0.9357	0.7119	0.6922	0.6879	0.6843	0.6804	1.4545	1.0403	0.9907	0.9751	0.9637	0.9535
	0.12	0	0.9471	0.7036	0.6798	0.6759	0.6732	0.6702	1.4697	1.0161	0.9569	0.9409	0.9305	0.9212
	0.18	0	0.9598	0.6919	0.6611	0.6569	0.6554	0.6538	1.4866	0.9834	0.9086	0.8909	0.8818	0.8742
	0.24	0	0.9739	0.6748	0.6314	0.6248	0.6240	0.6239	1.5054	0.9375	0.8334	0.8096	0.8012	0.7961
	0.30	0	0.9898	0.6490	0.5797	0.5624	0.5577	0.5566	1.5266	0.8689	0.6985	0.6460	0.6271	0.6194

Table 7. Natural frequencies of the SSSS and CCCG FGP (case 2) square nano-plate versus k and ξ .

Nonlocal factor (μ)	ξ	k	SSSS					CCCG						
			0	2	4	6	8	10	0	2	4	6	8	10
0	0	0	1.2171	0.9272	0.9018	0.8944	0.8878	0.8811	1.9954	1.4548	1.3900	1.3658	1.3473	1.3310
	0.06	0	1.2279	0.9298	0.9032	0.8962	0.8901	0.8839	2.0114	1.4546	1.3865	1.3621	1.3439	1.3280
	0.12	0	1.2392	0.9322	0.9040	0.8974	0.8919	0.8862	2.0280	1.4538	1.3816	1.3570	1.3392	1.3236
	0.18	0	1.2509	0.9343	0.9041	0.8979	0.8931	0.8880	2.0455	1.4522	1.3751	1.3502	1.3327	1.3176
	0.24	0	1.2632	0.9361	0.9033	0.8974	0.8933	0.8890	2.0637	1.4496	1.3665	1.3410	1.3240	1.3094
	0.30	0	1.2761	0.9374	0.9013	0.8955	0.8922	0.8887	2.0828	1.4458	1.3553	1.3288	1.3121	1.2981
1	0	0	1.1170	0.8550	0.8324	0.8259	0.8200	0.8141	1.7996	1.3144	1.2574	1.2363	1.2202	1.2060
	0.06	0	1.1270	0.8576	0.8339	0.8278	0.8224	0.8168	1.8141	1.3144	1.2543	1.2333	1.2175	1.2036
	0.12	0	1.1373	0.8600	0.8349	0.8292	0.8244	0.8193	1.8292	1.3138	1.2502	1.2290	1.2136	1.2001
	0.18	0	1.1482	0.8622	0.8354	0.8300	0.8258	0.8213	1.8450	1.3125	1.2446	1.2232	1.2082	1.1951
	0.24	0	1.1595	0.8641	0.8350	0.8299	0.8264	0.8225	1.8615	1.3104	1.2371	1.2152	1.2007	1.1881
	0.30	0	1.1714	0.8656	0.8336	0.8286	0.8258	0.8227	1.8788	1.3071	1.2272	1.2045	1.1904	1.1784
2	0	0	1.0393	0.7992	0.7788	0.7730	0.7678	0.7624	1.6518	1.2088	1.1574	1.1388	1.1244	1.1116
	0.06	0	1.0486	0.8018	0.7805	0.7750	0.7702	0.7652	1.6651	1.2090	1.1549	1.1362	1.1221	1.1097
	0.12	0	1.0583	0.8043	0.7817	0.7766	0.7723	0.7677	1.6790	1.2086	1.1513	1.1325	1.1189	1.1068
	0.18	0	1.0684	0.8066	0.7824	0.7776	0.7739	0.7699	1.6935	1.2075	1.1463	1.1274	1.1142	1.1025
	0.24	0	1.0790	0.8086	0.7824	0.7779	0.7748	0.7714	1.7087	1.2057	1.1397	1.1204	1.1076	1.0965
	0.30	0	1.0901	0.8103	0.7814	0.7770	0.7746	0.7719	1.7247	1.2029	1.1308	1.1109	1.0986	1.0880
4	0	0	0.9252	0.7179	0.7008	0.6961	0.6917	0.6871	1.4407	1.0589	1.0155	1.0000	0.9880	0.9772
	0.06	0	0.9336	0.7205	0.7026	0.6982	0.6943	0.6900	1.4524	1.0592	1.0136	0.9981	0.9865	0.9760
	0.12	0	0.9423	0.7231	0.7042	0.7001	0.6966	0.6928	1.4646	1.0592	1.0108	0.9954	0.9841	0.9740
	0.18	0	0.9514	0.7255	0.7053	0.7015	0.6985	0.6952	1.4773	1.0586	1.0069	0.9914	0.9805	0.9709
	0.24	0	0.9609	0.7277	0.7058	0.7023	0.6999	0.6971	1.4906	1.0573	1.0015	0.9858	0.9754	0.9662
	0.30	0	0.9708	0.7297	0.7055	0.7022	0.7003	0.6981	1.5046	1.0552	0.9943	0.9780	0.9681	0.9595

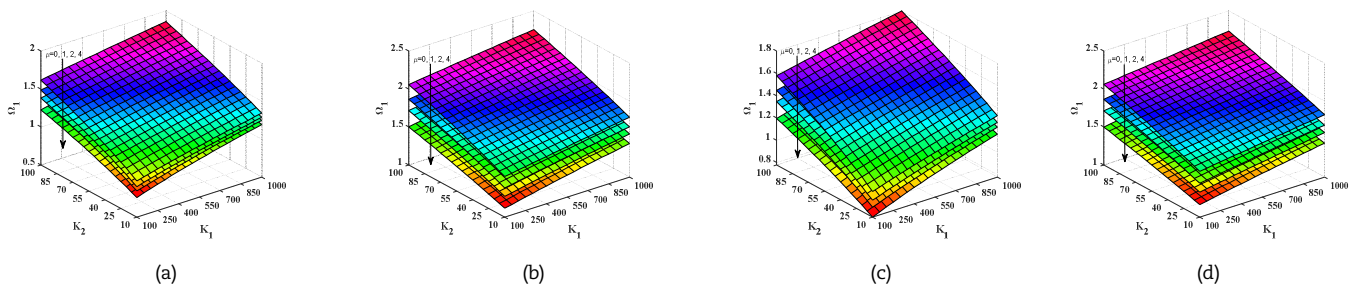


Fig. 11. Natural frequencies of FGP square nano-plate versus K_1 and K_2 . (a) The SSSS FGP (case 1) nano-plate. (b) The CCCG FGP (case 1) nano-plate. (c) The SSSS FGP (case 2) nano-plate. (d) The CCCG FGP (case 2) nano-plate.



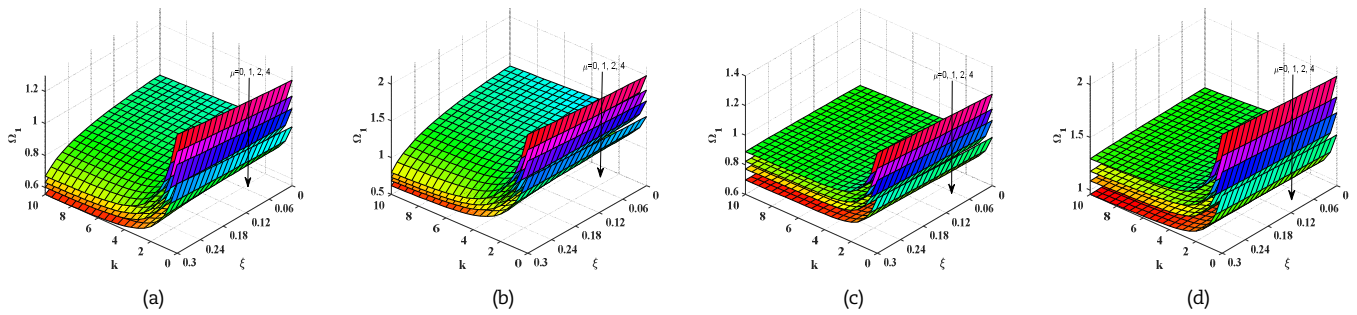


Fig. 12. Natural frequencies of FGP square nano-plate versus k and ξ . (a) The SSSS FGP (case 1) nano-plate. (b) The CCCC FGP (case 1) nano-plate. (c) The SSSS FGP (case 2) nano-plate. (d) The CCCC FGP (case 2) nano-plate.

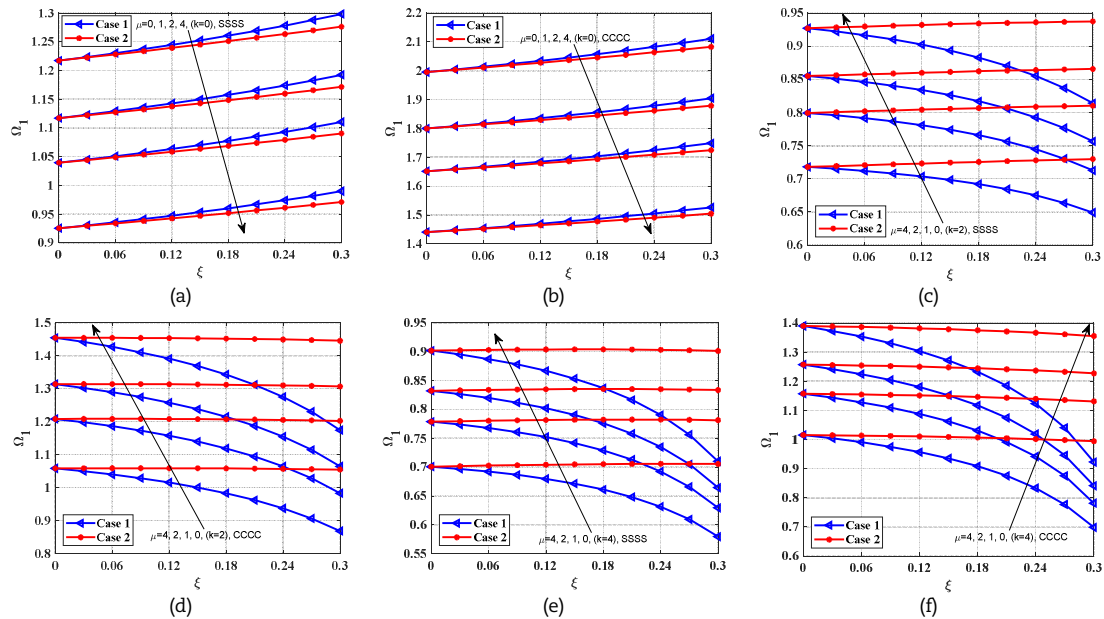


Fig. 13. Natural frequencies vibration of the FGP square nano-plate versus ξ . (a) The SSSS FGP nano-plate ($k = 0$). (b) The CCCC FGP nano-plate ($k = 0$). (c) The SSSS FGP nano-plate ($k = 2$). (d) The CCCC FGP nano-plate ($k = 2$). (e) The SSSS FGP nano-plate ($k = 4$). (f) The CCCC FGP nano-plate ($k = 4$).

5. Conclusion

In this paper, some new numerical results of the free vibration analysis of FGP nano-plates with different shapes on the EF are considered. The authors employed the Q8 element based on the FSDT to establish the fundamental equations. Our numerical results are in excellent agreement with other published articles. This work has the following advantages:

- Numerical methods are employed to compute the free vibration of FGP nano-plates with different shapes on the EF.
- Using the FEM easily mesh for complicated geometry domains, applying for analysis of structures with different boundary conditions, and other loads.
- The Q8 element converges faster than using the MITC4 element and the Q4 element in the free vibration problem of nano-plates.
- Employing the FSDT is simple in formulations and computational efficiency.
- The increase of elastic foundation stiffness k_1, k_2 leads to the increase in the stiffness of the FGP nano-plates.
- The material parameters k, ξ , and the porosity distribution affect significantly the free vibration of nano-plates. Basically, these two-parameters increases result in reducing the stiffness of nano-structures.
- The law of porosity distribution significantly effects the material property distribution through-thickness of the FGP nano-plate. Therefore, it effects the mechanical behavior of the nano-plate.
- These numerical results are useful for the calculation, design, and manufacturing technology.

Author Contributions

T.L. Doan and P.B. Le planned the research; T.T. Tran and Q.-H. Pham developed the calculation modeling and proposed analytical method. P.B. Le and V.K. Trai analyzed the results. The article was written and revised by all authors.

Conflict of Interest

The authors declared no potential conflicts of interest with respect to the research, authorship, and publication of this article.



Funding

The authors received no financial support for the research, authorship, and publication of this article.

References

- [1] Yang, F., A. Chong, D.C.C. Lam, and P. Tong, Couple stress based strain gradient theory for elasticity, *International Journal of Solids and Structures*, 39(10), 2002, 2731-2743.
- [2] Aifantis, E.C., *Strain gradient interpretation of size effects, Fracture scaling*, 299-314, Springer, New York, 1999.
- [3] Eringen, A.C., On differential equations of nonlocal elasticity and solutions of screw dislocation and surface waves, *Journal of Applied Physics*, 54(9), 1983, 4703-4710.
- [4] Eringen, A.C., *Nonlocal Continuum Field Theories*, Springer, New York, 2002.
- [5] Li, C., C. W. Lim, and J. Yu, Twisting statics and dynamics for circular elastic nanosolids by nonlocal elasticity theory, *Acta Mechanica Sinica*, 24(6), 2011, 484-494.
- [6] Ansari, R., S. Sahmani, and B. Arash, Nonlocal plate model for free vibrations of single-layered graphene sheets, *Physics Letters A*, 375(1), 2010, 53-62.
- [7] Arash, B., and Q. Wang, A review on the application of nonlocal elastic models in modeling of carbon nanotubes and graphenes, *Computational Materials Science*, 51(1), 2012, 303-313.
- [8] Asemi, S. R., and A. Farajpour, Decoupling the nonlocal elasticity equations for thermo-mechanical vibration of circular graphene sheets including surface effects, *Physica E: Low-dimensional Systems and Nanostructures*, 60, 2014, 80-90.
- [9] Jalali, S., E. Jomehzadeh, and N. Pugno, Influence of out-of-plane defects on vibration analysis of graphene: Molecular Dynamics and Non-local Elasticity approaches, *Superlattices and Microstructures*, 91, 2016, 331-344.
- [10] Aghababaei, R., and J. Reddy, Nonlocal third-order shear deformation plate theory with application to bending and vibration of plates, *Journal of Sound and Vibration*, 326(1-2), 2009, 277-289.
- [11] Pradhan, S., and T. Murmu, Small scale effect on the buckling of single-layered graphene sheets under biaxial compression via nonlocal continuum mechanics, *Computational Materials Science*, 47(1), 2009, 268-274.
- [12] Reddy, J., Nonlocal nonlinear formulations for bending of classical and shear deformation theories of beams and plates, *International Journal of Engineering Science*, 48(11), 2010, 1507-1518.
- [13] Pradhan, S.C., and Phadikar, J.K., Nonlocal theory for buckling of nano-plates, *International Journal of Structural Stability and Dynamics*, 11(3), 2011, 411-429.
- [14] Farajpour, A., M. Danesh, and M. Mohammadi, Buckling analysis of variable thickness nanoplates using nonlocal continuum mechanics, *Physica E: Low-dimensional Systems and Nanostructures*, 44(3), 2011, 719-727.
- [15] Murmu, T., and S. Adhikari, Nonlocal vibration of bonded double-nanoplate-systems, *Composites Part B: Engineering*, 42(7), 2011, 1901-1911.
- [16] Aksencer, T., and M. Aydogdu, Forced transverse vibration of nanoplates using nonlocal elasticity, *Physica E: Low-dimensional Systems and Nanostructures*, 44(7-8), 2012, 1752-1759.
- [17] Satish, N., S. Narendar, and S. Gopalakrishnan, Thermal vibration analysis of orthotropic nanoplates based on nonlocal continuum mechanics, *Physica E: Low-dimensional Systems and Nanostructures*, 44(9), 2012, 1950-1962.
- [18] Shen, Z.-B., H.-L. Tang, D.-K. Li, and G.-J. Tang, Vibration of single-layered graphene sheet-based nanomechanical sensor via nonlocal Kirchhoff plate theory, *Computational Materials Science*, 61, 2012, 200-205.
- [19] Hosseini-Hashemi, S., M. Zare, and R. Nazemnezhad, An exact analytical approach for free vibration of Mindlin rectangular nano-plates via nonlocal elasticity, *Composite Structures*, 100, 2013, 290-299.
- [20] Fazelzadeh, S. A., and E. Ghavanloo, Nanoscale mass sensing based on vibration of single-layered graphene sheet in thermal environments, *Acta Mechanica Sinica*, 30(1), 2014, 84-91.
- [21] Tran, T. T., Tran, V. K., Pham, Q.-H., and Zenkour, A. M, Extended four-unknown higher-order shear deformation nonlocal theory for bending, buckling and free vibration of functionally graded porous nanoshell resting on elastic foundation, *Composite Structures*, 264, 2021, 113737.
- [22] Tran, V.-K., Tran, T.-T., Phung, M.-V., Pham, Q.-H., and Nguyen-Thoi, T, A Finite Element Formulation and Nonlocal Theory for the Static and Free Vibration Analysis of the Sandwich Functionally Graded Nanoplates Resting on Elastic Foundation, *Journal of Nanomaterials*, 2020 2020, 8786373.
- [23] Liu, C., Yu, J., Xu, W., Zhang, X., and Wang, X, Dispersion characteristics of guided waves in functionally graded anisotropic micro/nano-plates based on the modified couple stress theory, *Thin-Walled Structures*, 161, 2021, 107527.
- [24] Phung-Van, P., and Thai, C. H, A novel size-dependent nonlocal strain gradient isogeometric model for functionally graded carbon nanotube-reinforced composite nanoplates, *Engineering with Computers*, 2021, 1-14, doi: 10.1007/s00366-021-01353-3.
- [25] Phung-Van, P., Lieu, Q. X., Nguyen-Xuan, H., and Wahab, M. A. Size-dependent isogeometric analysis of functionally graded carbon nanotube-reinforced composite nanoplates, *Composite Structures*, 166, 2017, 120-135.
- [26] Xinran, Z., M. Huang, A. Dongqi, C. Zhou, and R. Li, New analytic bending, buckling, and free vibration solutions of rectangular nanoplates by the symplectic superposition method, *Scientific Reports*, 11(1), 2021.
- [27] Ho, D. T., S.-D. Park, S.-Y. Kwon, K. Park, and S. Y. Kim, Negative Poisson's ratios in metal nanoplates, *Nature Communications*, 5(1), 2014, 1-8.
- [28] Ke, L.-L., Y.-S. Wang, J. Yang, and S. Kitipornchai, Free vibration of size-dependent magneto-electro-elastic nanoplates based on the nonlocal theory, *Acta Mechanica Sinica*, 30(4), 2014, 516-525.
- [29] Malekzadeh, P., M. G. Haghghi, and M. Shojaei, Nonlinear free vibration of skew nanoplates with surface and small scale effects, *Thin-Walled Structures*, 78, 2014, 48-56.
- [30] Lee, Z., C. Ophus, L. Fischer, N. Nelson-Fitzpatrick, K. Westra, S. Evoy, V. Radmilovic, U. Dahmen, and D. Mitlin, Metallic NEMS components fabricated from nanocomposite Al-Mo films, *Nanotechnology*, 17(12), 2006, 3063.
- [31] Simsek, M., Nonlocal effects in the free longitudinal vibration of axially functionally graded tapered nanorods, *Computational Materials Science*, 61, 2012, 257-265.
- [32] Simsek, M., and H. Yurtcu, Analytical solutions for bending and buckling of functionally graded nanobeams based on the nonlocal Timoshenko beam theory, *Composite Structures*, 97, 2013, 378-386.
- [33] Natarajan, S., S. Chakraborty, M. Thangavel, S. Bordas, and T. Rabczuk, Size-dependent free flexural vibration behavior of functionally graded nanoplates, *Computational Materials Science*, 65, 2012, 74-80.
- [34] Nazemnezhad, R., and S. Hosseini-Hashemi, Nonlocal nonlinear free vibration of functionally graded nanobeams, *Composite Structures*, 110, 2014, 192-199.
- [35] Hosseini-Hashemi, S., I. Nahas, M. Fakher, and R. Nazemnezhad, Surface effects on free vibration of piezoelectric functionally graded nanobeams using nonlocal elasticity, *Acta Mechanica*, 225(6), 2014, 1555-1564.
- [36] Hosseini-Hashemi, S., R. Nazemnezhad, and M. Bedroud, Surface effects on nonlinear free vibration of functionally graded nanobeams using nonlocal elasticity, *Applied Mathematical Modelling*, 38(14), 2014, 3538-3553.
- [37] Natarajan, S., S. Chakraborty, M. Thangavel, S. Bordas, and T. Rabczuk, Size-dependent free flexural vibration behavior of functionally graded nanoplates, *Computational Materials Science*, 65, 2012, 74-80.
- [38] Jung, W.-Y., and S.-C. Han, Analysis of sigmoid functionally graded material (S-FGM) nanoscale plates using the nonlocal elasticity theory, *Mathematical Problems in Engineering*, 2013, 2013.
- [39] Nami, M. R., M. Janghorban, and M. Damadam, Thermal buckling analysis of functionally graded rectangular nanoplates based on nonlocal third-order shear deformation theory, *Aerospace Science and Technology*, 41, 2015, 7-15.
- [40] Hosseini-Hashemi, S., M. Bedroud, and R. Nazemnezhad, An exact analytical solution for free vibration of functionally graded circular/annular Mindlin nanoplates via nonlocal elasticity, *Composite Structures*, 103, 2013, 108-118.
- [41] Salehipour, H., H. Nahvi, and A. Shahidi, Exact analytical solution for free vibration of functionally graded micro/nanoplates via three-dimensional nonlocal elasticity, *Physica E: Low-dimensional Systems and Nanostructures*, 66, 2015, 350-358.
- [42] Salehipour, H., A. Shahidi, and H. Nahvi, Modified nonlocal elasticity theory for functionally graded materials, *International Journal of Engineering Science*, 90, 2015, 44-57.



- [43] Ansari, R., M. F. Shojaei, A. Shahabodini, and M. Bazdid-Vahdati, Three-dimensional bending and vibration analysis of functionally graded nanoplates by a novel differential quadrature-based approach, *Composite Structures*, 131, 2015, 753-764.
- [44] Wang, Y.-Z., and F.-M. Li, Static bending behaviors of nanoplate embedded in elastic matrix with small scale effects, *Mechanics Research Communications*, 41, 2012, 44-48.
- [45] Narendar, S., and S. Gopalakrishnan, Nonlocal continuum mechanics based ultrasonic flexural wave dispersion characteristics of a monolayer graphene embedded in polymer matrix, *Composites Part B: Engineering*, 43(8), 2012, 3096-3103.
- [46] Pouresmaeeli, S., E. Ghavanloo, and S. Fazelzadeh, Vibration analysis of viscoelastic orthotropic nanoplates resting on viscoelastic medium, *Composite Structures*, 96, 2013, 405-410.
- [47] Zenkour, A., and M. Sobhy, Nonlocal elasticity theory for thermal buckling of nanoplates lying on Winkler-Pasternak elastic substrate medium, *Physica E: Low-dimensional Systems and Nanostructures*, 53, 2013, 251-259.
- [48] Daikh, A. A., and A. M. Zenkour, Bending of Functionally Graded Sandwich Nanoplates Resting on Pasternak Foundation under Different Boundary Conditions, *Journal of Applied and Computational Mechanics*, 6(S1), 2020, 1245-1259.
- [49] Ebrahimi, F., A. Dabbagh, and T. Rabczuk, On wave dispersion characteristics of magnetostrictive sandwich nanoplates in thermal environments, *European Journal of Mechanics-A/Solids*, 85, 2021, 104130.
- [50] Panyatong, M., B. Chinnaboon, and S. Chucheeepsakul, Incorporated effects of surface stress and nonlocal elasticity on bending analysis of nanoplates embedded in an elastic medium, *Suranaree J. Sci. Technol.*, 22(1), 2015, 21-33.
- [51] Anitescu, C., E. Atroshchenko, N. Alajlan, and T. Rabczuk, Artificial neural network methods for the solution of second order boundary value problems, *Computers, Materials and Continua*, 59(1), 2019, 345-359.
- [52] Guo, H., Zhuang, X., and Rabczuk, T., A deep collocation method for the bending analysis of Kirchhoff plate, *Computers, Materials & Continua*, 59, 2019, 433-456.
- [53] Samaniego, E., C. Anitescu, S. Goswami, V. M. Nguyen-Thanh, H. Guo, K. Hamdia, X. Zhuang, and T. Rabczuk, An energy approach to the solution of partial differential equations in computational mechanics via machine learning: Concepts, implementation and applications, *Computer Methods in Applied Mechanics and Engineering*, 362, 2020, 112790.
- [54] Vu-Bac, N., T. Lahmer, X. Zhuang, T. Nguyen-Thoi, and T. Rabczuk, A software framework for probabilistic sensitivity analysis for computationally expensive models, *Advances in Engineering Software*, 100, 2016, 19-31.
- [55] Zhuang, X., H. Guo, N. Alajlan, H. Zhu, and T. Rabczuk, Deep autoencoder based energy method for the bending, vibration, and buckling analysis of Kirchhoff plates with transfer learning, *European Journal of Mechanics-A/Solids*, 87, 2021, 104225.
- [56] Shahsavari, D., M. Shahsavari, L. Li, and B. Karami, A novel quasi-3D hyperbolic theory for free vibration of FG plates with porosities resting on Winkler/Pasternak/Kerr foundation, *Aerospace Science and Technology*, 72, 2018, 134-149.
- [57] Reddy, J.N., *Mechanics of laminated composite plates and shells: theory and analysis*, CRC press, 2003.
- [58] Thai, H.-T., and D.-H. Choi, A refined plate theory for functionally graded plates resting on elastic foundation, *Composites Science and Technology*, 71(16), 2011, 1850-1858.
- [59] Roque, C., D. Cunha, C. Shu, and A. Ferreira, A local radial basis functions-Finite differences technique for the analysis of composite plates, *Engineering Analysis with Boundary Elements*, 35(3), 2011, 363-374.
- [60] Thai, C.H., H. Nguyen-Xuan, S. P. A. Bordas, N. Nguyen-Thanh, and T. Rabczuk, Isogeometric analysis of laminated composite plates using the higher-order shear deformation theory, *Mechanics of Advanced Materials and Structures*, 22(6), 2015, 451-469.

Appendix


The Lagrange interpolation in Eq. (34):


$$\psi_1 = \frac{1}{4}(1-\zeta)(1-\eta)(-\zeta-\eta-1); \quad \psi_2 = \frac{1}{2}(1-\zeta^2)(1-\eta); \quad \psi_3 = (1+\zeta)(1-\eta)(-\zeta-\eta-1); \quad \psi_4 = \frac{1}{2}(1+\zeta)(1-\eta^2);$$


$$\psi_5 = \frac{1}{4}(1+\zeta)(1+\eta)(\zeta+\eta-1); \quad \psi_6 = \frac{1}{2}(1-\zeta^2)(1+\eta); \quad \psi_7 = \frac{1}{4}(1-\zeta)(1+\eta)(-\zeta+\eta-1); \quad \psi_8 = \frac{1}{2}(1-\zeta)(1-\eta^2)$$


where ζ, η are natural coordinates.


ORCID iD

Trac Luat Doan  <https://orcid.org/0000-0003-1531-5163>

Pham Binh Le  <https://orcid.org/0000-0003-2023-6275>

Trung Thanh Tran  <https://orcid.org/0000-0002-1730-0590>

Vu Khac Trai  <https://orcid.org/0000-0003-3693-6022>

Quoc Hoa Pham  <https://orcid.org/0000-0001-6316-3120>



© 2021 Shahid Chamran University of Ahvaz, Ahvaz, Iran. This article is an open access article distributed under the terms and conditions of the Creative Commons Attribution-NonCommercial 4.0 International (CC BY-NC 4.0 license) (<http://creativecommons.org/licenses/by-nc/4.0/>).

How to cite this article: Doan T.L., Le P.B., Tran T.T., Trai V.K., Pham Q.H. Free Vibration Analysis of Functionally Graded Porous Nano-plates with Different Shapes Resting on Elastic Foundation, *J. Appl. Comput. Mech.*, 7(3), 2021, 1593-1605. <https://doi.org/10.22055/JACM.2021.36181.2807>

Publisher's Note Shahid Chamran University of Ahvaz remains neutral with regard to jurisdictional claims in published maps and institutional affiliations.

